Structural characterization and *in vitro* bioactivity assessment of SiO_2–CaO–P_2O_5–SrO–Al_2O_3 glass as bioactive ceramic material

5.1 Introduction

Bioactive glasses have the ability to dissolve in physiological fluids, releasing hydrated-silica and ions such as Na^+, Ca^{2+} and PO_4^{3-}. The precipitation of these species leads to a silicon rich hydrated gel layer and hydroxy-carbonated apatite (HCA) formation. The HCA is the mineral component of the bone and tooth, thus bioactive glasses have been studied as potential candidates for medical and dental applications. These glasses are commercially available as bone substitute materials and as a remineralising additive for toothpastes. The first bioactive glass known as 45S5 Bioglass® was developed by Hench (Hench, 1993). Its composition is 46.1 SiO_2–2.5 P_2O_5–24.4 Na_2O–26.9 CaO (mol%). Since then, several new bioactive glass compositions have been developed, which are of interest for use as bone grafts (Hench, 1998), implant coatings(Gomez *et al*., 2000 and Lotfibakhshaiesh *et al*., 2010), bone cements (Towler *et al*., 2002) and even in dentifrices (Tai *et al*., 2006). It has been shown that in 45S5 Bioglass® (SiO_2–P_2O_5–CaO–Na_2O) SrO can be substituted for calcium oxide due to their similar ionic radii of 0.94Å (Ca^{2+}) and 1.16Å (Sr^{2+}) (O'Donnell *et al*., 2010). The small difference in size allows the substitution of the strontium for calcium ions not only in glass composition but also in crystal lattices (O'Donnell *et al*., 2008). However, it is important to emphasize that due to the difference in atomic weight (the Sr (88) is more than twice that of the atomic weight

of Ca (40)), it makes more useful to substitute SrO for calcium oxide not on a weight basis but on a molar basis, which was mentioned in detail by O'Donnell and Hill (O'Donnell *et al*., 2010).

A significant challenge is posed for regeneration of large size bone defects generally caused due to infections, trauma, accidents, tumors or genetic malformations in the human body. It necessitates the need for effective materials of bone regeneration and tissue engineering capability. Various grafting materials are being utilized today in an attempt to repair osseous defects. The use of these materials is based on the assumption that they possess osteogenic potential, and are osteoconductive (able to support bone formation) or osteoinductive (able to induce bone formation) (Wang *et al*., 2005). Multifunctional bioactive glasses offer an excellent opportunity in delivering therapeutic ions like strontium (Sr^{2+}) (Wu *et al*., 2012, Wu and Chang, 2014, Fuchs *et al*., 2015), a trace element in human body.

Despite their similarity, Sr^{2+} ion has got certain advantages which Ca^{2+} does not have. Sr^{2+} ions have been shown to stimulate osteoblastic bone formation and to inhibit osteoclastic bone resorption both *in vitro* and *in vivo* (Bonnelye *et al*., 2008, Marie *et al*., 1993 and Habibovic *et al*., 2011). Indeed strontium ranelate (Protelos®) is a drug approved for treatment and prevention of osteoporosis (Marie, 2005 and O'Donnell *et al*., 2006) whilst Sr-containing bioactive glasses were shown to combine the known bone regenerative properties of bioactive glasses with the anabolic and anti-catabolic effects of Sr^{2+} cations *in vitro* (Gentleman *et al*., 2010). Strontium is an important source of interest in recent years because of its effect on bone cells. Strontium is one of the alkaline earth metals and like calcium it is a bone-seeking agent. Strontium is naturally present in the

liver, muscles and physiological fluids but is mainly present in bone. However, the amount of strontium in bone is typically only 3.5% of its calcium content. It is preferentially found in new bones rather than old and more in cancellous than cortical bones. Both *in vitro* and *in vivo* studies have demonstrated stimulatory effects of Sr on osteoblasts and an inhibitory effect on osteoclasts, associated with an increase in bone density and resistance (Marie *et al.*, 1993, Canalis *et al.*, 1996, Baron *et al*., 2002 and Bonnelye *et al.*, 2008). Nowadays, strontium ranelate is used as a commercial antiosteoporoticoral drug that has been proven to reduce the incidence of fractures in osteoporotic patients (Meunier *et al.*, 2004, Reginster *et al.*, 2008).

Moreover, these bioactive glasses possess low mechanical strength which may be a hindrance for repairing defects especially in load-bearing bones. In recent years several attempts were made to tailor the degradation rate and to improve the mechanical strength of bioactive glasses by changing their chemical composition and with the incorporation of various other metal oxides like MgO, ZnO, B_2O_3, Al_2O_3, etc. in to the base bioactive glass. Amongst several oxides the addition of Al_2O_3 to the bioactive glass is expected to improve the long-time stability of the implants needed for bone defect repairing (El-Kheshen *et al*., 2008) and to control the degradation rate. The studies on the influence of aluminium on the crystallization and bioactivity of $NaCaPO_4$–SiO_2 system by Sitarz *et al*. (Sitarz *et al*., 2010) have indicated that addition of Al^{3+} ion in appropriate proportion increases the mechanical resistance of the bioglasses, influences homogeneity of the glass texture and dramatically changes the composition of the matrix and inclusions. However, the addition of Al_2O_3 in large quantities to the borate free silicate-based bioactive glass is not desirable because of its carcinogenicity and adverse impact on the bioactivity of the

glass (Ohtsuki *et al*., 1992 and Gross *et al*., 1985). However, the role of Al_2O_3 for SrO in the past has never been investigated in such systems. The incorporation of SrO has been shown to be useful in bioactive glasses without influencing their bioactivity and increasing bone regeneration and tissue engineering capability. Therefore, in the present investigation, the concentration of SrO was varied with molar addition of Al_2O_3 from 0.5% to 2.5%. The idea for assessment of *in vitro* bioactivity in simulated body fluid (SBF), physico-chemical, mechanical properties as well as cell culture of the glasses has been also undertaken herewith. It is expected that the bioactivity and physico-mechanical properties would be improved significantly with increasing the concentration of Al_2O_3 in the base bioactive glass. Furthermore, an *in vitro* cell culture studies, like cell viability and cytotoxicity have been extensively investigated for better conclusions. Interestingly, it can be seen as follows that all the samples are tolerant to white blood cells (WBC) and RBC causing no significant loss of viability or hemolysis.

5.2 Materials and methods

5.2.1 Sample preparation

Glass samples were prepared in five different compositions by taking the starting materials as reagent grade fine-grained quartz (SiO_2), analytical reagent grade calcium carbonate ($CaCO_3$), ammonium dihydrogen phosphate ($(NH_4)H_2PO_4$), strontium carbonate ($SrCO_3$) in the required stoichiometric ratio in mol% (Table 5.1). The required amount of analytical reagent grade Al_2O_3 was added in each batch for the partial substitution of SrO. The raw materials for different samples were properly weighed. The mixing of different batches was done for 30 min and then after that, the raw batches were

melted in a 100 ml platinum-2% rhodium crucible for 4h kept in a globar electric furnace at 1400°C in air atmosphere. The temperature of the furnace was controlled with in ± 10°C by an automatic temperature indicator-cum-controller. Further, the glass melt was taken out of the furnace, poured on an aluminum sheet in a rectangular mold and transferred immediately to an annealing furnace. The glass samples were properly annealed at 500°C for 1h and cooled slowly to room temperature with a controlled rate of cooling inside the muffle furnace to remove the thermal stress and strain from the glass. A part of the annealed bioactive glass samples was cut, ground and polished for measurement of its physical and mechanical properties.

Table 5.1 Mol% compositions of the bioactive glass samples.

Sl. No.	SAMPLE	SiO_2	CaO	P_2O_5	SrO	Al_2O_3	Al_2O_3 / SrO ratio
1.	Sr-1	42	34	6	18	0	0.00
2.	Sr-2	42	34	6	17.5	0.5	0.028
3.	Sr-3	42	34	6	17	1.0	0.058
4.	Sr-4	42	34	6	16.5	1.5	0.090
5.	Sr-5	42	34	6	15.5	2.5	0.161

The other parts of the samples were crushed in a pestle mortar and then ground in an agate mortar to make fine powders for measurements of its bioactivity and other properties using various experimental techniques such as XRD, FTIR spectrometry, SEM analysis and pH measurements. The *in vitro* cell culture studies were also performed with the bioactive glass samples against human osteosarcoma cells U2-OS.

5.2.3 X-ray diffraction analysis

The powdered samples were subjected to X-ray diffraction analysis using a Rigaku portable XRD machine (Rigaku, Tokyo, Japan) (40kV, 20 mA) from 20° to 80° in steps of 0.018. The Cu Kα radiation with Ni filtered was used for X-ray analysis. Phase identification was carried out by comparing the XRD patterns of the bioactive glass samples with the standard database stated by JCPDS X-ray diffraction card files.

5.3 Results and discussion

5.3.1 Mechanical properties

5.3.1.1 Density and compressive strength

Figs. 5.1 and 5.2 show the density and compressive strength of the glass samples as a function of Al_2O_3/SrO ratio within error bars.

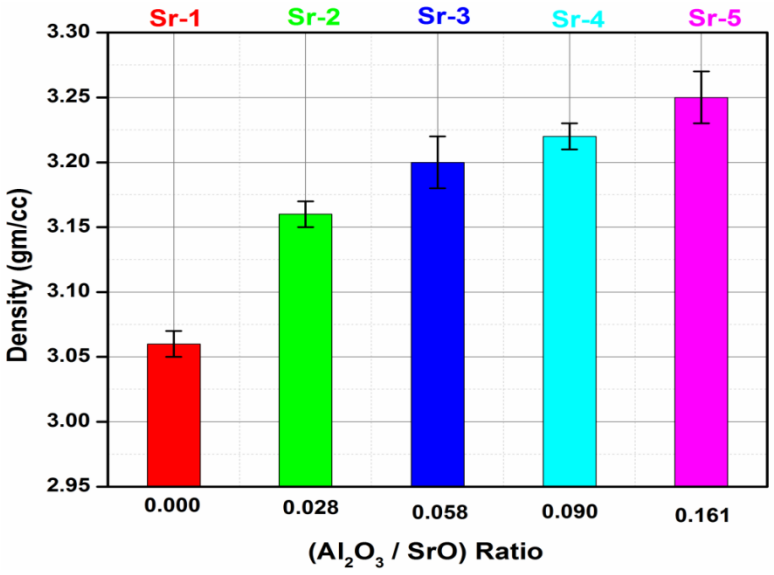

Fig. 5.1: Variation in density with Al_2O_3/SrO ratio in bioactive glass samples Sr-1 to Sr-5.

It is clear from Figs. 1 and 2 that an increase in Al2O3/SrO ratio with increasing Al2O3 substitution resulted in an increase in the density and the compressive strength of glass samples from 2.74 to 2.79 gm/cc and 58 to 69 MPa. This is attributed due to the reason that the Al^{3+} ions might have occupied interstitial sites within the glass network (Muller *et al*., 1983 and Brow *et al*., 1997). Earlier magic angle spinning-nuclear magnetic resonance (MAS NMR) studies on the glasses containing ^{27}Al indicated that aluminum ions occupy both tetrahedral sites with AlO_4 (viz., substitutional or network forming positions) and octahedral with AlO_6 (viz., interstitial or network modifiers) structural units (Brow *et al*., 1997). However, previous studies have also pointed out that AlO_6 dominates the glass structure when Al_2O_3 is present in low concentrations, whereas AlO_4 structural units prevail when Al_2O_3 content is higher (Belkebir *et al*., 1999).

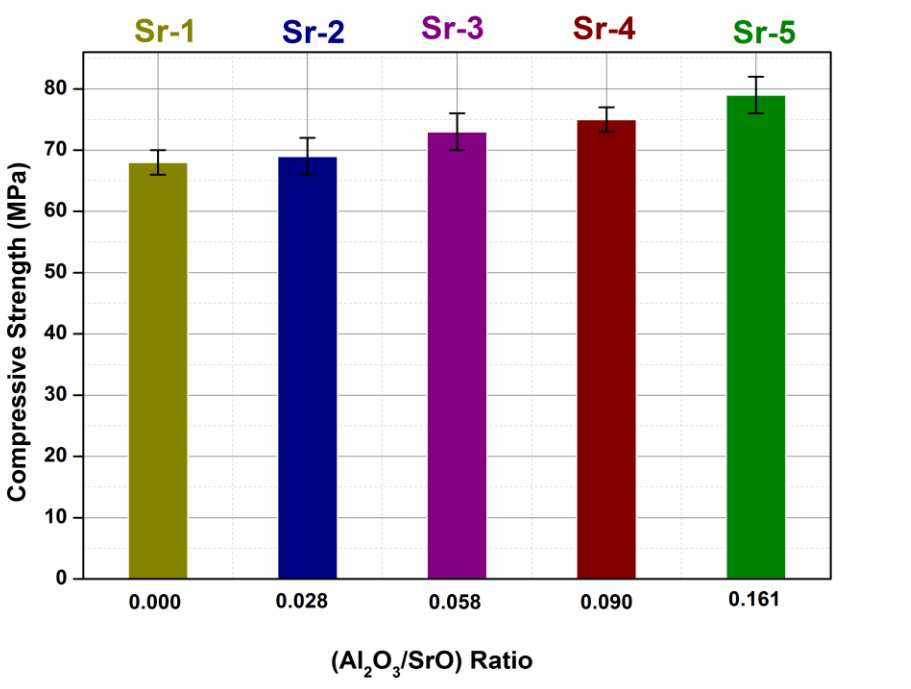

Fig.5.2: Variation in compressive strength with Al_2O_3/SrO ratio in bioactive glass samples Sr-1 to Sr-5.

Therefore, it increased the densities and resulted in creating new bonds with incorporation of Al^{3+} ions in the bioactive glasses. It has caused the reinforcement of glass structure and resulted in an improvement in the compression of the glass samples.

5.3.1.2 Modulus of elasticity

Fig. 5.3 represents the experimental values of elastic moduli such as Young's modulus (E), shear modulus (S) and bulk modulus (K) of the bioactive glass samples with increasing Al_2O_3/SrO ratio. All the elastic moduli values were found to increase with increasing Al_2O_3/SrO ratio. The elastic moduli of the bioactive glass samples have shown similar trends regarding improvement in their mechanical properties with the variation in the ultrasonic velocities.

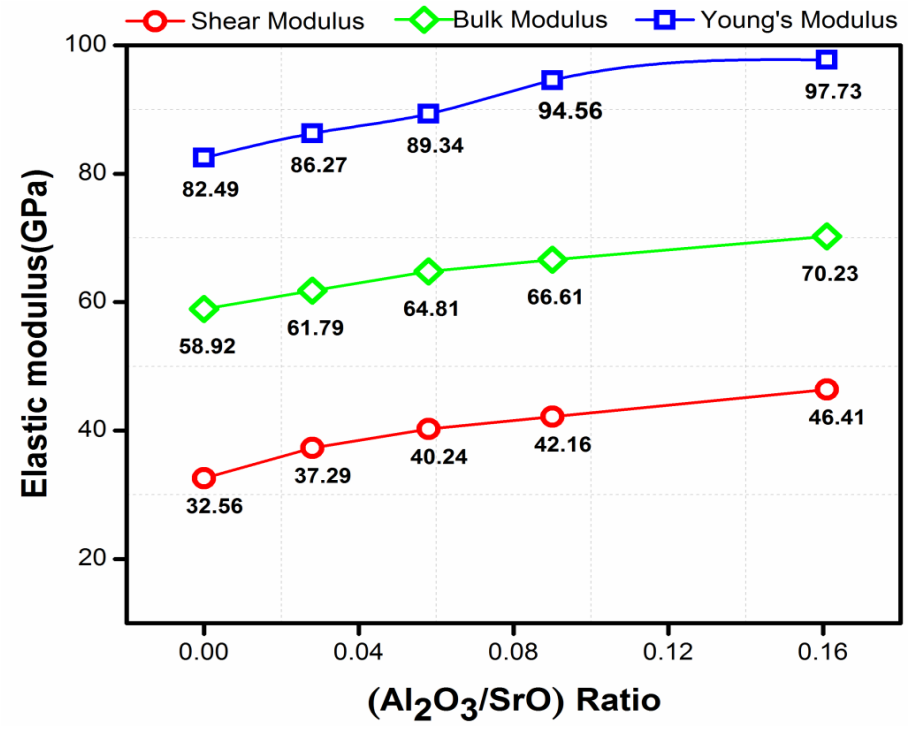

Fig. 5.3: Elastic modulus, shear modulus and bulk modulus of all bioactive glass samples Sr-1 to Sr-5.

The modifiers like Mg^{2+}, Ca^{2+} and Sr^{2+} etc. occupy the interstitial positions in the glass structure (Hill and Brauer, 2011 and Gaafar *et al*., 2013). As the concentration of SrO increases the compactness of the glass structure also increases. Therefore, the average number of the network bonds per unit volume increases in the glass structure (Rajendran *et al*., 2002, Vallet-Reg *et al*., 2005, Gaafar *et al*., 2013). Hence, the propagation of sound wave in compacted glass could be much faster which resulted in the improvement in longitudinal and shear wave velocities and there by thus increase in elastic modulus. Moreover, it was observed from earlier studies (Rajendran *et al*., 2002 and Vallet-Reg *et al*., 2005) that glasses containing higher amount of modifiers have shown better mechanical strength. Similarly, the incremental addition of Al_2O_3 at the cost of SrO increases the modifier's concentration in the bioactive glass and this has revealed a significant increase in elastic moduli of these bioactive glasses.

5.3.2 pH behavior

Fig. 5.4 shows the variation of pH of SBF solution after immersing bioactive glass samples into it up to 28 days. It shows that for all bioactive glass samples, the pH increases within 1 to 7 days as compared to the initial pH of the SBF solution at 7.4 and 37°C temperature under physiological condition. The mechanism of HCA formation can be assessed by the pH behavior of SBF after immersion of the samples (Hench 1991, Hench 2005, Balamurugan *et al*., 2007) in the solution. The pH of SBF increased significantly from an initial value of 7.20 to 8.18, 8.32, 8.39, 8.27 and 8.12 for Sr-1, Sr-2, Sr-3, Sr-4 and Sr-5, respectively after 3 days of immersion. An appreciable increase in pH demonstrates the dissolution of cations from the surface of the glass. The high pH leads to an attack on silica network and formation of silanols. After three days

immersion, the pH of the SBF decreased in all the samples, which was due to the absorption of calcium and phosphate ions from the SBF to promote the HCA layer formation on the surface of the samples (Silver *et al*., 2001, Hench 2005). After fourth day immersion and onwards pH remained almost constant due to the migration of amorphous $CaO\text{-}P_2O_5$ rich film by incorporation of soluble calcium and phosphates from the solution (Goel *et al*., 2011). This leads to attack on the silica glass network, which results silanols formation leading to decrease in pH as indicated in Fig. 5.4 when bioactive glass samples were immersed in SBF solution for 7 to 28 days.

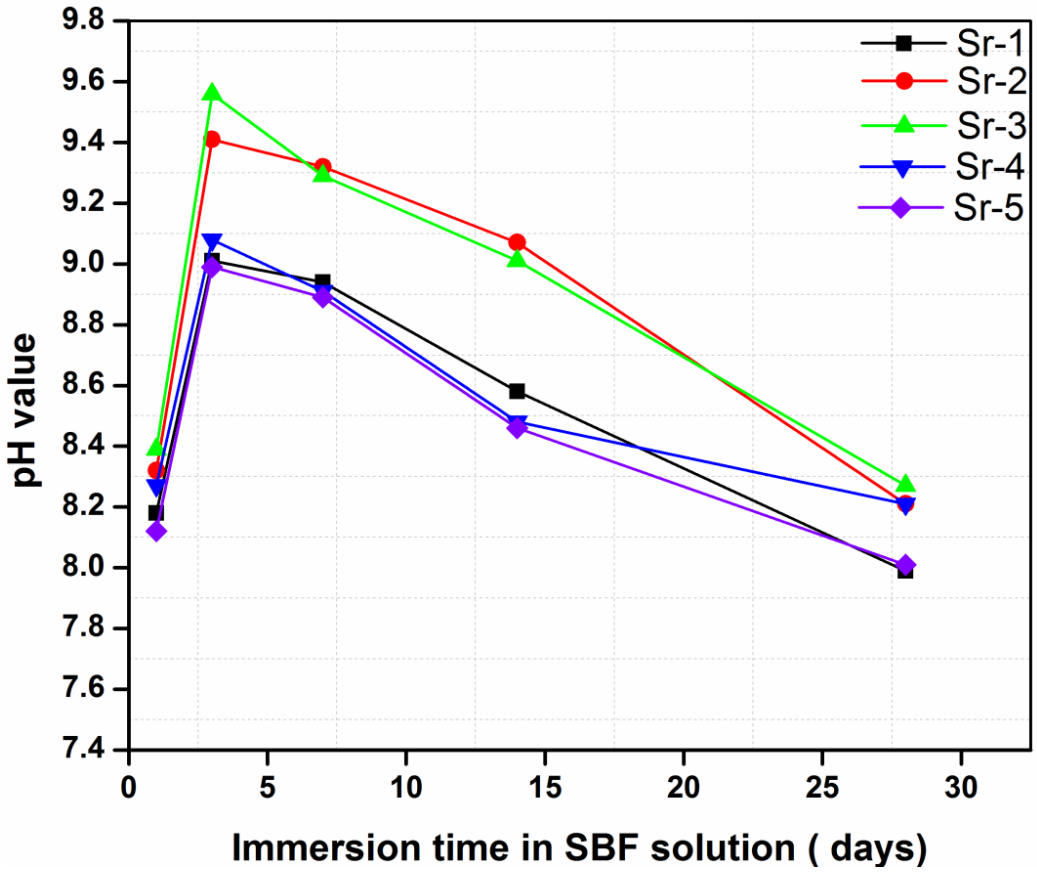

Fig. 5.4: Variation of pH of bioactive glass samples (Sr-1 to Sr-5) after immersing in simulated body fluid (SBF) up to 28 days.

It was also seen that the decrease in the pH of the SBF solution after 14 days was due to breaking of glass network. Fig. 5.4 shows that addition of alumina up to 1.5 mol%, results in an increase in pH of the SBF solution containing immersed samples which attained maxima after around three days and then it decreased with time referring to base glass sample. However, the addition of Al_2O_3 beyond this (> 1.5–2.5 mol%) up to 2.5 mol% caused a decrease in maxima of the pH of the SBF solution containing immersed sample. This dictates that addition of Al_2O_3 up to 1.5 mol% in the glass samples has increased its bioactivity, but beyond 1.5 mol% up to 2.5 mol% of Al_2O_3 retards the bioactivity of the glass samples (Fig. 5.4). This observation can be explained in the manner that addition of Al_2O_3 up to 1.5 mol% goes into formation of AlO_6 octahedra and produces more of non-bridging oxygens which results in an increase in bioactivity of samples. Whereas further addition of Al_2O_3 beyond 1.5 mol%, results in the formation of AlO_4 tetrahedra which causes a decrease in the bioactivity of the samples (Belkebir *et al*., 1999, Zhao *et al*., 2009 and Brow *et al*., 1997). Therefore, the results demarcate that the substitution of Al_2O_3 for SrO in the present investigation did not alter the bioactivity mechanism in SBF.

5.3.4 *In vitro* bioactivity of bioactive glasses by X-ray diffractometry

Fig. 5.5 represents the XRD pattern of prepared bioactive glass samples (Sr-1, Sr-2, Sr-3, Sr-4 and Sr-5). The investigation was carried here for the qualitative characterization of bioactive glasses. It is evident from the XRD data that all the bioactive glasses were homogeneous and amorphous in nature. The bulk glasses were optically transparent after melting and casting. Notably, the amorphous scattering of a broad hump at 2 θ around

32° was found in all the glasses and this hump became more intense as the concentration of Al_2O_3 increased in Sr-3, Sr-4 and Sr-5 glass samples.

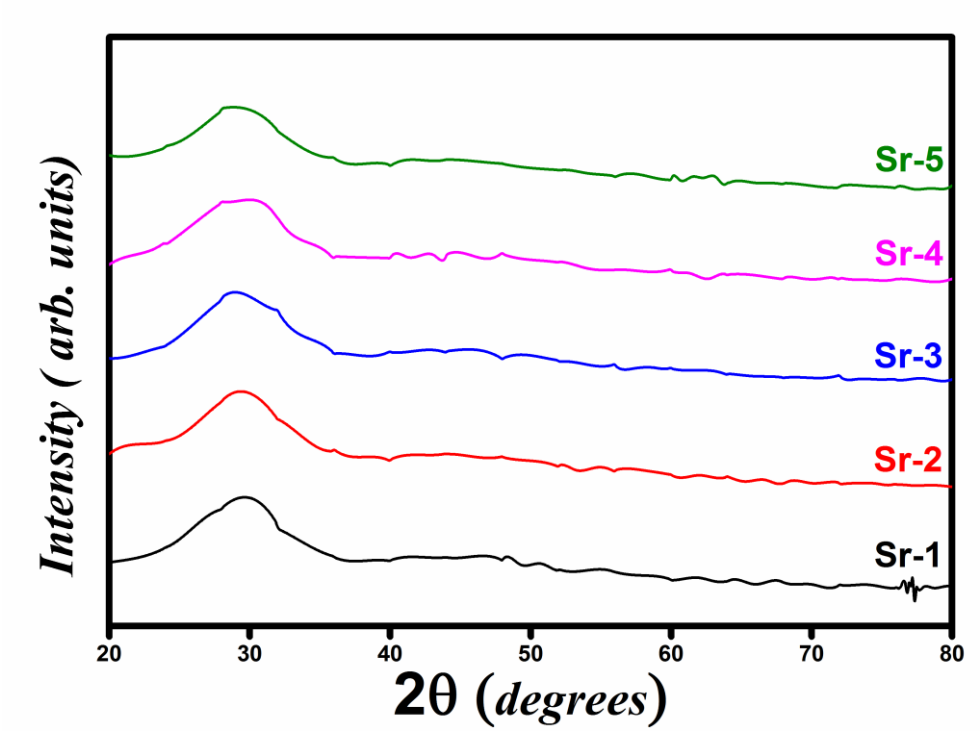

Fig. 5.5: XRD patterns of the bioactive glass samples (Sr-1 to Sr-5) before soaking them into the simulated body fluid (SBF) solution.

This change may be attributed due to narrowing of the silicate network by larger alumina cations (Fredholm *et al.*, 2010). Fig. 5.6 shows the XRD patterns of the bioactive glasses after immersion in SBF for 14days and the results show the formation of crystalline phases after SBF treatment. In general, the bioactivity of the samples is associated with the ability of hydroxy apatite (HA) layer formation on their surface in SBF under physiological conditions. The *hkl* planes (211), (203) and (313) are located at 2 θ corresponding to crystalline phase of hydroxyapatite [$Ca_{10}(PO_4)_6(OH)_2$] and the

diffraction peaks were matched with the standard PCPDF#: 74-0565 (Chen *et al*., 2006, Balamurugan *et al*., 2007, Arepalli *et al*., 2015).

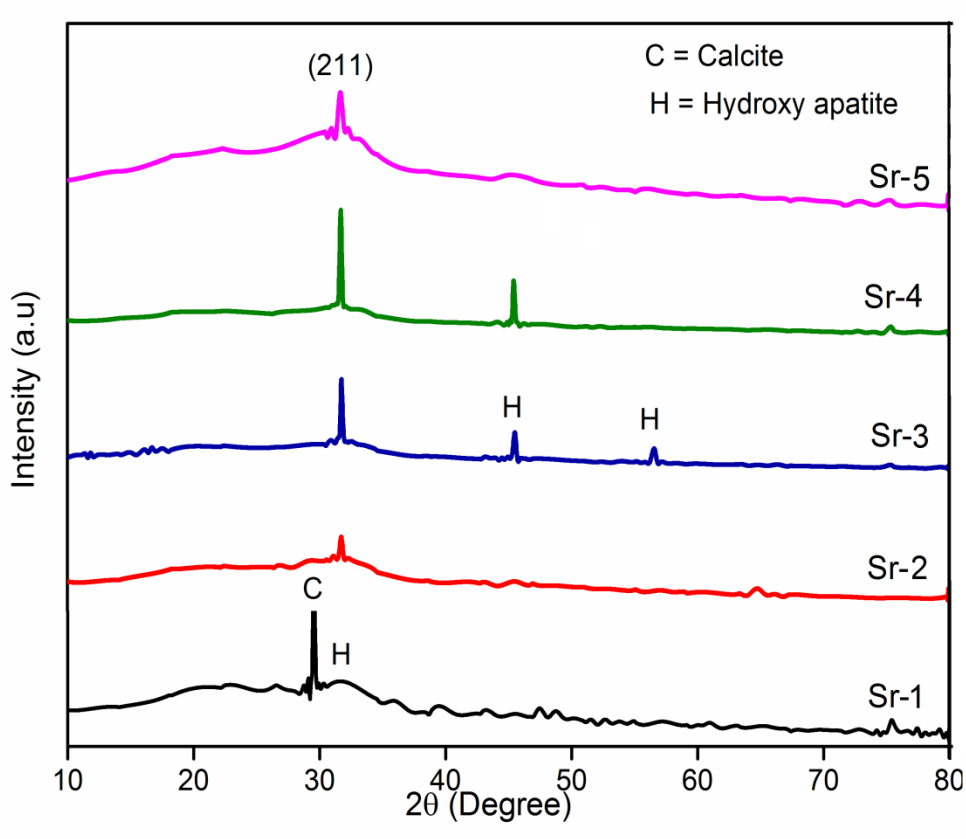

Fig. 5.6: XRD patterns of the bioactive glass samples (Sr-1 to Sr-5) soaked in the simulated body fluid (SBF) solution for 14 days.

Therefore, all the samples confirm the HA phase formation after immersion in SBF for 14 days. It was observed from the XRD patterns that the intensities of the peak (211) differed with each other and this difference is attributed due to the varying amount of phase formed in each sample. Therefore, the present system favours the HCA formation which has been also proved by the SEM and FTIR spectrometry as shown in Fig. 5.7, 5.8 and next Figs. 5.9–5.13, respectively.

5.3.5 SEM analysis of bioactive glass samples

The SEM micrographs of bioactive glass samples before soaking in SBF solution have been shown in Fig. 5.7 (a)–(e) which shows different rod type structures and irregular grains of bioactive glass samples similar to the results observed by Hanan *et al*. (Hanan *et al*., 2009).

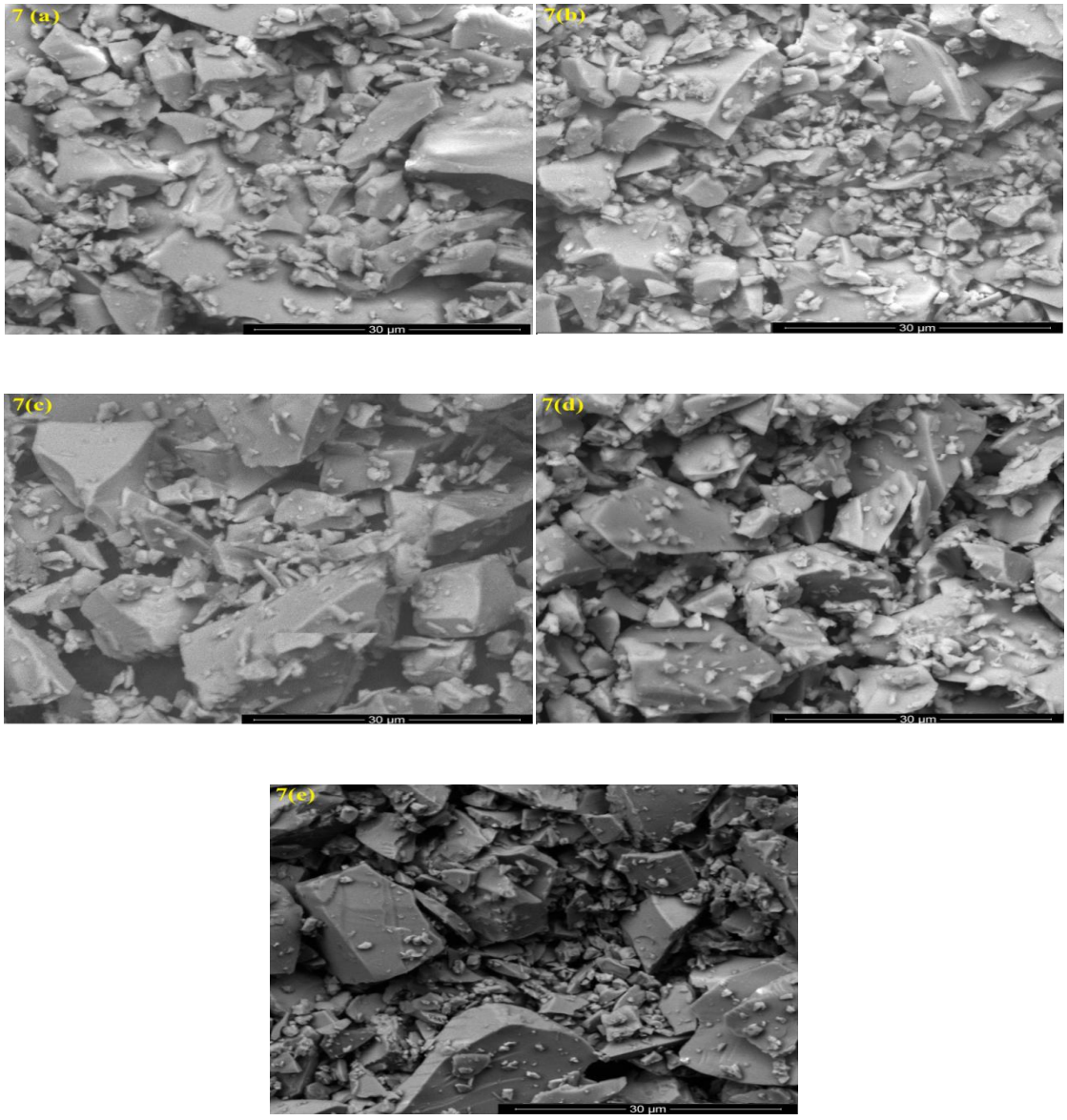

Fig. 5.7(a–e): SEM micrographs of bioactive glass samples (Sr-1 to Sr-5) before soaking in SBF solution.

This happens due to solution refreshing and demonstrating the formation of a continuous layer of HCA (Verne *et al*., 2005). Fig.5.8 (a)–(e) shows the SEM micrographs of bioactive glass samples after soaking in SBF solution for 28 days.

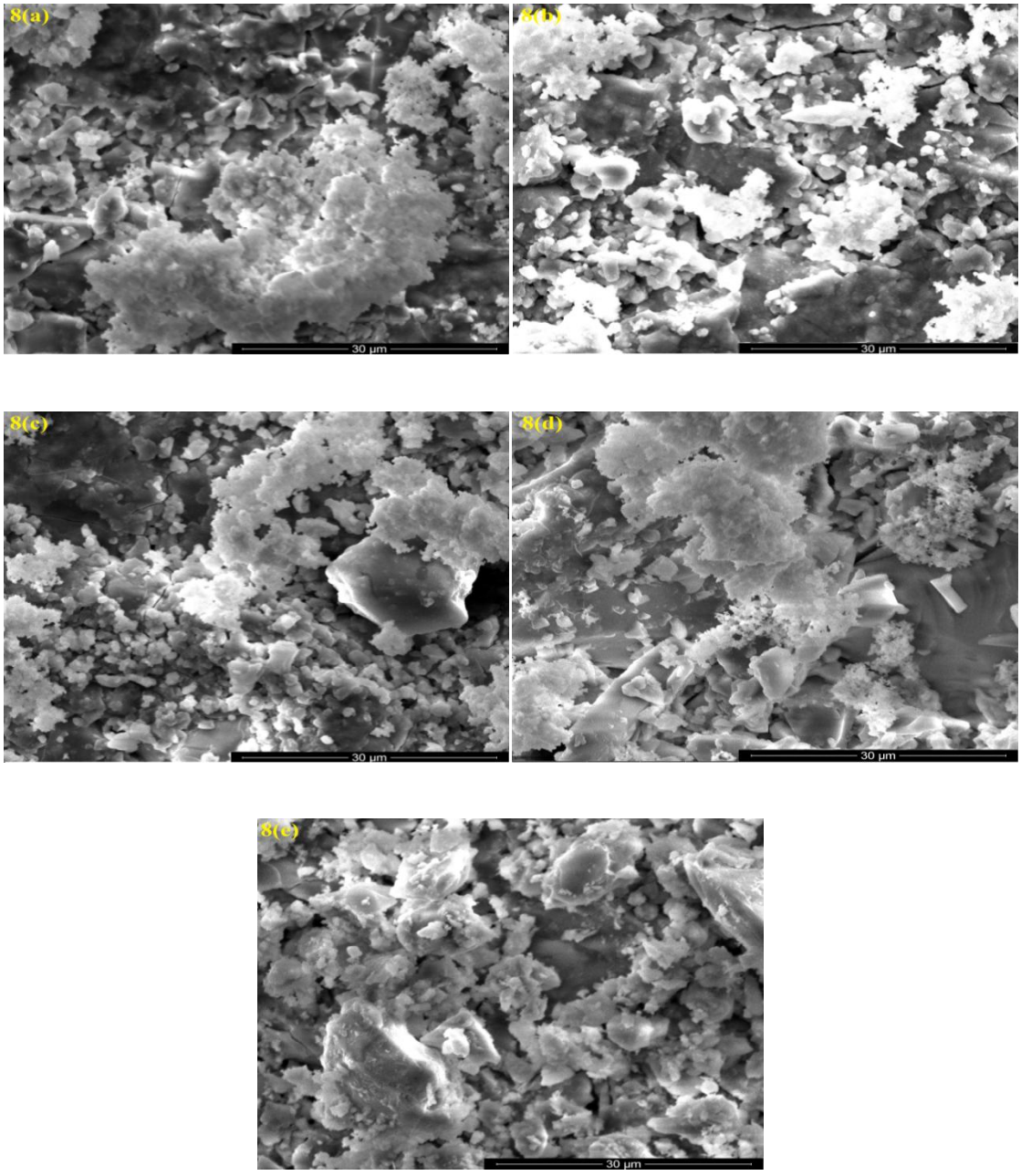

Fig. 5.8(a–e): SEM micrographs of bioactive glass samples (Sr-1 to Sr-5) which were soaked in SBF solution for 28 days.

A change in surface morphology is seen if it is compared with the initial surface of the bioactive glass samples. The SEM micrographs demonstrate that spherical particles have covered the surface of the bioactive glasses with variable shape and size. Therefore, the SEM pictures further confirm the growth of HCA layer on the surface of the samples after immersing in SBF solution. On SBF treatment, HCA clusters change in a finer structure after 28 days of soaking due to partial dissolution and re-precipitation phenomena in solution. So, after comparing these micrographs it can be concluded that the micrographs have shown the formation of HCA on the surface of bioactive glass samples after immersion in SBF solution for 28 days. It was also observed that the numbers of HCA crystals are more on the surface of Sr-2, Sr-3 and Sr-4 samples as compared with other bioactive glasses. This significant development of HCA crystals might be associated with an appreciable high deposition of Ca-P layer and it is in good agreement with the XRD data (Fig. 5.6). Higher amount of Al_2O_3 in Sr-5 causes a decrease in the formation of HCA as compared to other glass samples. So, for a better bioactivity of these glass samples the amount of alumina should be limited up to 1.5 mol% because the addition of Al_2O_3 in larger quantities in bioactive glass was not desirable due to its carcinogenicity and adverse impact on the bioactivity of glass (Mohini *et al*., 2013).

5.3.6 FTIR-spectrometry

Fig. 5.9 shows the Fourier transform infrared (FTIR) absorption spectra of the bioactive glass samples recorded in the wavenumber range of 400–4000 cm^{-1} on the FTIR spectrometer.

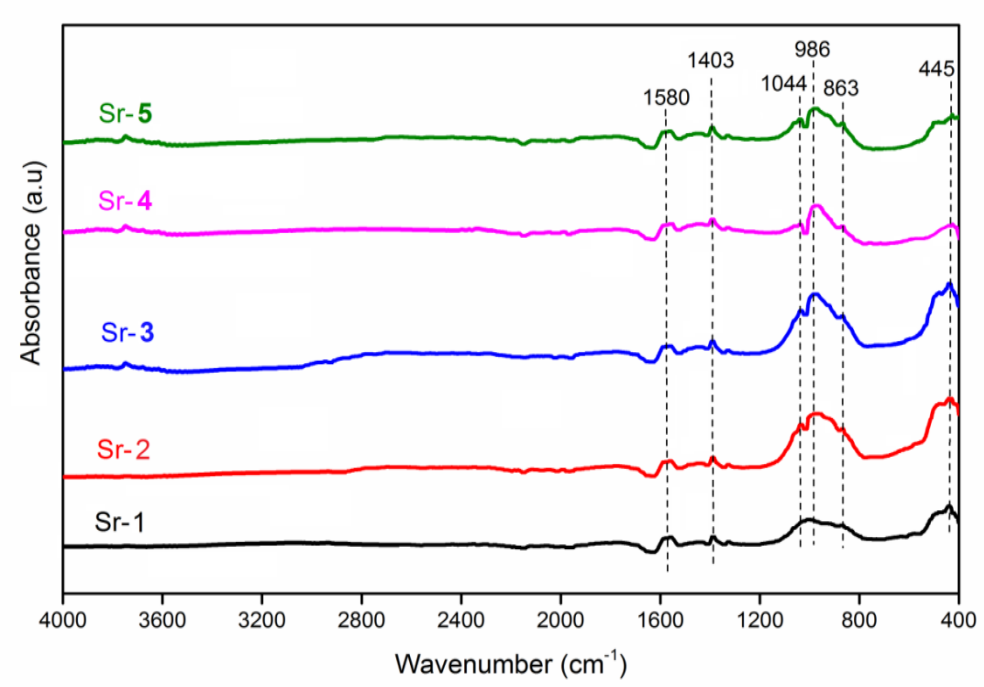

Fig. 5.9: FTIR absorption spectra of all the glass samples (Sr-1 to Sr-5) before soaking them into SBF solution.

The base bioglass (Sr-1) has revealed the FTIR peaks at 445, 863, 986, 1044, 1403 and 1580 cm^{-1}. The spectral absorption bands of Sr-2, Sr-3, Sr-4 and Sr-5 samples have revealed a similar behavior like Sr-1 sample, with small variations in the band intensities. The resultant FTIR band centered at around 445 cm^{-1} is associated with a Si–O–Si symmetric bending mode of vibration or AlO_6 octahedra and the peak at about 863 cm^{-1} is assigned due to the Si-O stretching mode of vibration. The minor peak observed at 1044 cm^{-1} can be attributed to Si-O-Si asymmetric stretching mode of vibration in the silicate tetrahedral network. The bands at 1403 cm^{-1} and 1580 cm^{-1} correspond to C-O stretching mode which might have appeared due to reaction between the glass and carbon dioxide present in the atmosphere (Fredholm *et al*., 2010). However, this phase was not noticed in the XRD pattern.

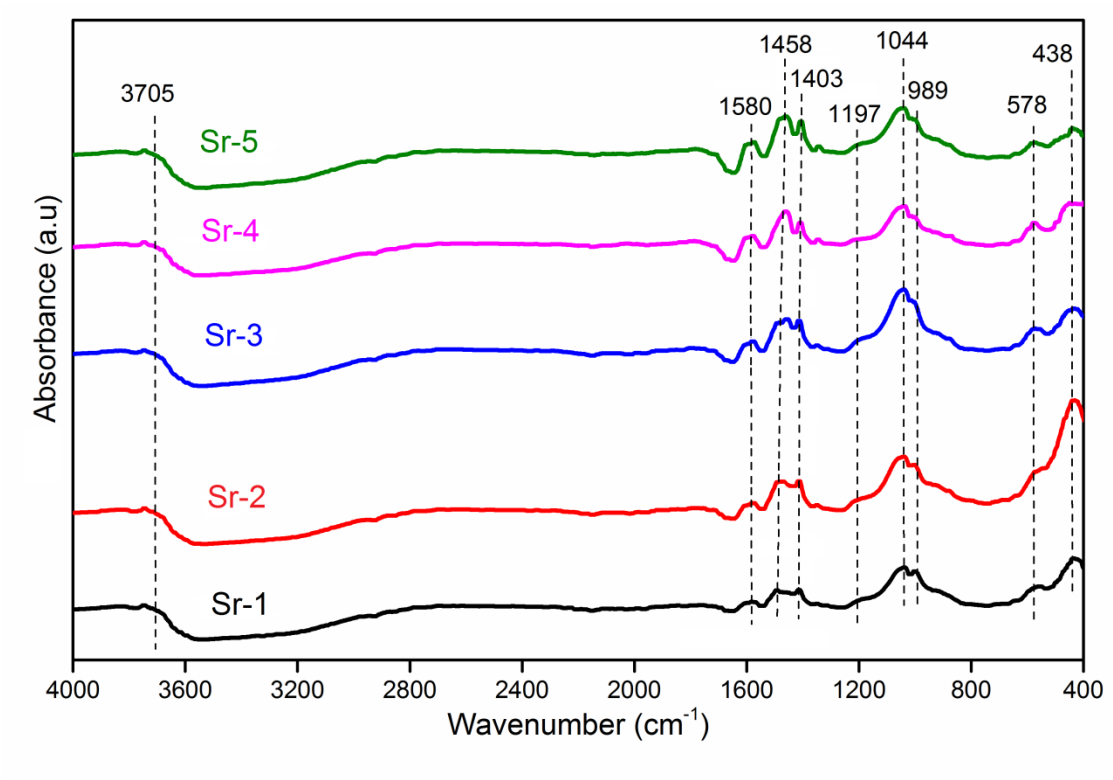

Fig. 5.10: FTIR absorption spectra of all the glass samples (Sr-1 to Sr-5) after soaking them into SBF for 14 days.

After immersion of the samples in SBF for 14 days, the new bands emerged at 578 cm^{-1}, 1197 cm^{-1}, 1458 cm^{-1} and 3705 cm^{-1} which are shown in Fig. 5.10. The bands centered at 578 cm^{-1} and 1197 cm^{-1} are attributed to the P-O bending mode of vibrations. An another new band appeared at around 1458 cm^{-1} corresponding to C-O stretching mode of vibration and broad band at around 3705 cm^{-1} is assigned to the presence of O-H groups. These characteristic bands represent the formation of hydroxyl carbonate apatite (HCA) layer on the surface of the bioactive glass samples (Romeis *et al*., 2014). It is noteworthy that the bands at 863 cm^{-1} and 986 cm^{-1} disappeared after immersion in SBF which is possibly due to the release of cations and simultaneous release of soluble silica from the samples. Therefore, the surface is rich in silica (Si-OH) layer and hence the band

intensity increased at 1044 cm^{-1} after SBF treatment and this peak became more prominent. It is quite evident from the spectra that the intensities of the carbonate (CO_3) groups (1403 cm^{-1} and 1458 cm^{-1}) have increased in these bioactive glasses (Chickerur *et al*., 1980). Therefore, the results suggest that the HCA layer formation on the surface of glass samples has taken place.

5.3.7 Measurement of cell viability, cell proliferation and cytotoxicity

The *in vitro* cell culture studies were carried out using human osteosarcoma U2-OS cell lines and assessment of the cell viability, cytotoxicity, proliferation, attachment and blood compatibility was done which are associated to biocompatibility. In general, most of the biomaterials at lower concentrations can exhibit biocompatibility in cell culture studies *in vitro*. Therefore, at higher concentration and longer duration experiments yield better information and conclusions for the compositional effect. Hence, I have performed the biological studies (cell viability, proliferation and blood compatibility) for prolonged time periods with various concentrations of the samples.

Cell viability of the bioactive glass samples (Sr-1, Sr-2, Sr-3, Sr-4 and Sr-5) was assessed against U2-OS cell lines by XTT viability assay. Fig. 5.11 (a) shows the percentage cell viability with different concentrations of the samples incubated for 24 h at 37°C in 5% CO_2. Bioactive glass samples do not affect the viability of U2-OS cells in short term as well as in long term interaction. U2-OS cells remain viable after and live following co-culture with glass samples (25 mg/ml) for 72 hours ($p>0.05$) (Fig. 5.11A). The percent cell viability was calculated by considering the viability of tumor cell cultured in complete medium only as 100%.

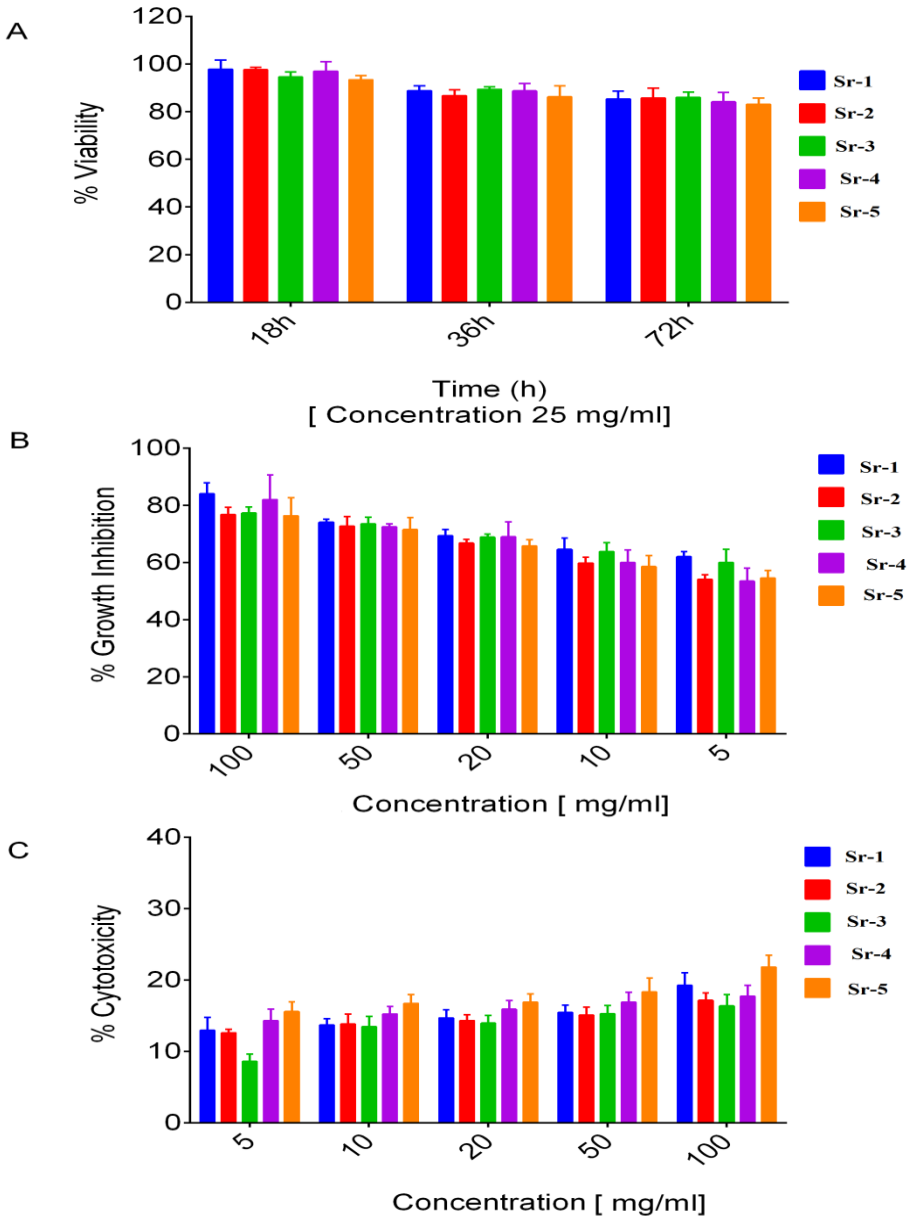

Fig. 5.11: (A) XTT Viability of U2-OS cells in the presence of fixed concentration (25 mg/ml) of bioactive glass sample. (B) Anti-proliferative effect of increasing concentrations of bioactive glass sample against U2-OS cells assessed by MTT assay. (C) Direct cytotoxicity of U2-OS cells in presence of increasing concentrations of bioactive glass samples.

U2-OS tumor cells remain healthy similar to that of untreated control cells following the treatment with bioactive glass samples (Sr-1 to Sr-5). The glass samples also had no effect on the proliferation of U2-OS cells at all the concentrations tested. A slight reduction in cell proliferation was recorded at highest concentration (100 mg/ml), although it remained non significant corresponding to the control (Fig. 5.11 B). The cell viability and proliferation data suggest that glass samples (Sr-1 to Sr-5) are tolerant to U2-OS cells with no significant loss of cell viability and proliferative capacity by the tumor cells. Higher concentration (100 mg/ml) of the samples exhibits slightly elevated levels of toxicity although that remains non significant (Fig. 5.11C). This is in good agreement with the earlier reports that the strontium containing bioactive glasses have exhibited cytocompatibility (Gorustovich *et al*., 2010, Hesaraki *et al*., 2010, Gentleman *et al*., 2010, O' Donnell *et al*., 2010 and Isaac *et al*., 2011). The cell viability and cytotoxicity data suggest that bioactive glass samples Sr-1 to Sr-5 are relatively tolerant to U2-OS cells which cause marginal or no loss of cell viability and direct cellular cytotoxicity.

5.3.8 Effect on normal cells

Similar to U2-OS cells, normal human RBC and PBMC were unaffected by the bioactive glass samples (Sr-1 to Sr-5). The glass samples do not cause any significant hemolysis of RBC (Fig. 5.12 A). The percent hemolysis never exceeds 2.0% following time dependent kinetic study at a fixed concentration.

Similar to RBC, fresh PBMC from normal donor also remained unaffected by the glass samples with no significant loss of viability in response to all the concentrations tested (Fig. 5.12B).

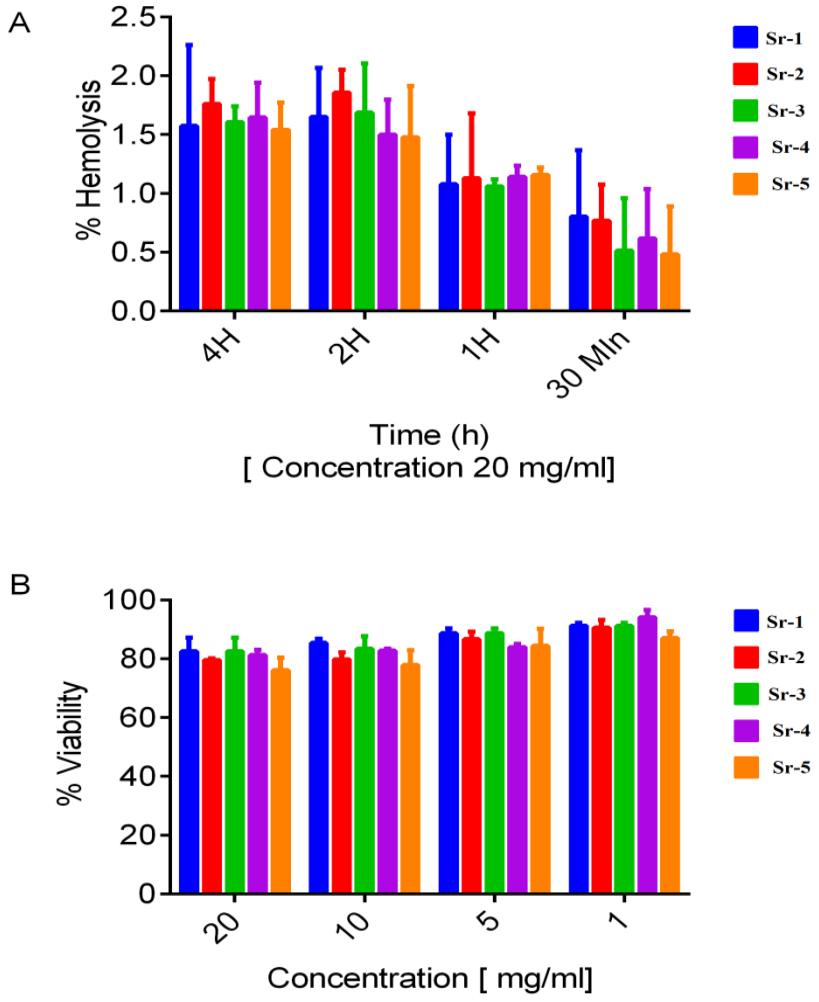

Fig. 5.12: (A) Lack of hemolysis in RBC by bioactive glass samples (Sr-1 to Sr-5) in time dependent kinetic study. (B) Viability of PBMC studied by XTT assay in presence varying concentrations of indicated samples.

5.3.9 Culture of U2-OS cells on bioactive glass samples

Fig. 5.13 (a-e) shows the SEM micrograph of the surfaces of bioactive glass samples after culturing with U2-OS cell lines for 5 days.

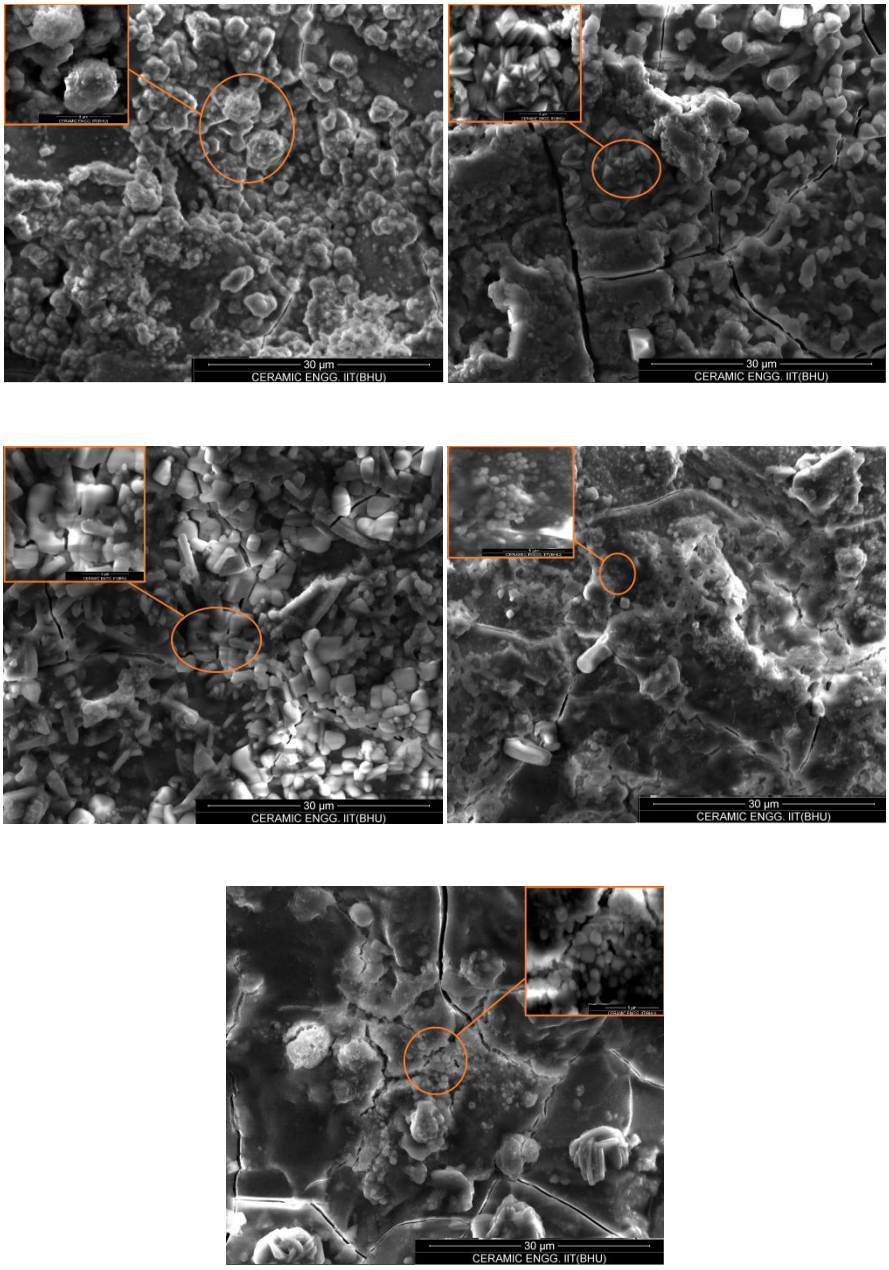

Fig. 5.13: SEM micrographs of U2-OS cells growth on biocompatible glass samples (Sr-1 to Sr-5).

I cultured the U2-OS cells on the bioactive glass samples in order to demonstrate the biocompatibility of the materials for possible clinical applications. U2-OS cells were grown in complete medium on the surface of the rectangular blocks of bioactive glasses in 24 well plates. Previously it has been also observed that there was an excellent attachment and spreading of cells on the surfaces of the bioactive glasses (Ding *et al*., 2009). All the samples except Sr-5 were found to exhibit a significant cell attachment and growth on their surfaces. It is well known that substitution of a modifier for a network former is highly favorable in cell attachment. However, if the amount of alumina is higher then it acts as a network former and it reduces the bioactivity. This might be the probable reason why there is less cell attachment in Sr-5 samples. It was also reported earlier that the Sr-contained HA layer had exhibited superior biological response *in vitro* and *in vivo* both (Wong *et al*., 2004 and Ni *et al*., 2006). This is in conformity to cell viability, cytotoxicity and cell attachment data of previous workers and the present results are well supported by their observations.

5.4 Conclusion

The present study with the SiO_2–CaO–P_2O_5–SrO–Al_2O_3 based bioactive glasses suggests that the material could be used in bone replacement for clinical cases. FTIR absorption spectra, pH behaviour, XRD and SEM images indicated the formation of hydroxyl carbonate apatite layer on the surface of the bioglasses after immersion in simulated body fluid. The density, compressive strength and elastic moduli were found to be enhanced with an increase in alumina content in the base bioglass. Alumina substituted bioactive glasses are biocompatible and exhibits marginal or no toxicity against epithelium of human osteosarcoma and RBC as well as mononuclear cells derived from peripheral

blood. These glass samples support the growth of the cells without causing any significant loss of viability and cell death. Osteosarcoma cells were found to grow on the surface of bioglasses which make the glass samples biocompatible and fit for use.

References:

Balamurugan A, Balossier G and Kannan S, Development and in vitro characterization of sol-gel derived CaO-P_2O_5-SiO_2-ZnO bioglass, Acta Biomater, 3, 255–262, 2007.

Baron R and Tsouderos Y, *In vitro* effects of S12911-2 on osteoclast function and bone marrow macrophage differentiation, Eur J Pharmacol, 450, 11-17, 2002.

Belkebir A, Rocha J, Esculcas AP, Berthet P, Gilbert BZ and Gabelica, Structural characterisation of glassy phases in the system Na_2O–Al_2O_3–P_2O_5 by MAS and solution NMR, EXAFS and vibrational spectroscopy, Spectrochimica Acta, 55, 1323–1336, 1999.

Bonnelye E, Chabadel A, Saltel F and Jurdic P, Dual effect of strontium ranelate: stimulation of osteoblast differentiation and inhibition of osteoclast formation and resorption in vitro, Bone, 42, 129–138, 2008.

Brow RK and Tallant DR, Structural design of sealing glasses, Journal of Non-Crystalline Solids, 222, 396–406, 1997.

Canalis E, Hott M, Deloffre P, Tsouderos Y and Marie PJ, The divalent strontium salt S12911 enhances bone cell replication and bone formation *in vitro*, Bone, 18, 517-523, 1996.

Chen QZ, Thompson ID and Boccaccini AR, 45S5 Bioglass-derived glass-ceramic scaffolds or bone tissue engineering, Biomaterials, 27, 2414–25, 2006.

Chickerur NS, Tung MS and Brown WE, A mechanism for incorporation of carbonate into apatite, Calcified Tissue International, 32, 55–62, 1980.

Ding S, Shie M and Wang C, Novel fast-setting calcium silicate bone cements with high

bioactivity and enhanced osteogenesis in vitro, J Mater Chem, 19, 1183, 2009.

El-Kheshen A, Khaliafa FA, Saad EA and Elwan RL, Effect of Al_2O_3 addition on bioactivity, thermal and mechanical properties of some bioactive glasses, Ceramic International, 34, 1667–1673, 2008.

Fredholm YC, Karpukhina N, Law RV and Hill RG, Strontium containing bioactive glasses: Glass structure and physical properties, Journal of Non-Crystalline Solids, Elsevier BV, 2546–2551, 2010.

Fuchs M, Gentleman E, and Shahid S, Therapeutic Ion-Releasing Bioactive Glass Ionomer Cements with Improved Mechanical Strength and Radiopacity, Front Mater, 2, 1–11, 2015.

Gaafar MS, Marzouk SY and Zayed HA, Structural studies and mechanical properties of some borate glasses doped with different alkali and cobalt oxides, Curr Appl Phys, 13, 152–158, 2013.

Gentleman E, Fredholm YC, Jell G, Lotfibakhshaiesh N, O'Donnell MD and Hill RG, The effects of strontium substituted bioactive glasses on osteoblasts and osteoclasts in vitro, Biomaterials, 31, 3949–3956, 2010.

Goel A, Rajagopal RR and Ferreira JMF, Influence of strontium on structure, sintering and biodegradation behaviour of $CaO\text{-}MgO\text{-}SrO\text{-}SiO_2\text{-}P_2O_5\text{-}CaF_2$ glasses, Acta Biomater, 7, 4071–4080, 2011.

Gomez-Vega JM, Saiz E, Tomsia A P, Oku T, Suganuma K and Marshall GW, Novel bioactive functionally graded coatings on Ti_6Al_4V, Adv Mater, 12, 894–898, 2000.

Gorustovich AA, Steimetz T, Cabrini RL and Porto López JM, Osteoconductivity of strontium-doped bioactive glass particles: a histomorphometric study in rats, J Biomed Mater Res A, 92, 232–237, 2010.

Gross U and Strunz V, The interface of various glasses and glass ceramics with a bony implantation bed, Journal of Biomedical Materials Research, 19, 251–271, 1985.

Habibovic P and Barralet JE, Bioinorganics and biomaterials: bone repair, Acta Biomater, 7, 3013–3026, 2011.

Hanan H Beherei, Khaled R Mohamed and Gehan T El-Bassyouni, Fabrication and characterization of bioactive glass (45S5)/titania biocomposites, Ceram Int, 35, 1991–1997, 2009.

Hench LL, Bioceramics: from concept to clinic, J Am Ceram Soc, 74, 1487–1510, 1991.

Hench LL, An introduction to bioceramics, World Scientific Publishing Company, Singapore, 1993.

Hench LL, Bioceramics, J Am Ceram Soc, 81, 1705–1728, 1998.

Hesaraki S, Alizadeh M, Nazarian H and Sharifi D, Physico-chemical and *in vitro* biological evaluation of strontium/calcium silicophosphate glass, J Mater Sci Mater Med, 21, 695–705, 2010.

Hill RG and Brauer DS, Predicting the glass transition temperature of bioactive glasses from their molecular chemical composition, Acta Biomater, 7, 3601–3605, 2011.

Isaac J, Nohra J and Lao J, Effects of strontium-doped bioactive glass on the differentiation of cultured osteogenic cells, Eur Cell Mater, 21, 130–143, 2011.

Lotfibakhshaiesh N, Brauer DS and Hill RG, Bioactive glass engineered coatings for Ti6Al4V alloys: influence of strontium substitution for calcium on sintering behaviour, J Non-Cryst Solids, 356, 2583–2590, 2010.

Marie PJ, Hott M, Modrowski D, Depollak C, Guillemain J and Deloffre P, An uncoupling agent containing strontium prevents bone loss by depressing bone-resorption and maintaining bone formation in estrogen-deficient rats, J Bone Miner Res, 8, 607–615, 1993.

Marie P J, Strontium as therapy for osteoporosis, Curr Opin Pharmacol, 5, 633–636, 2005.

Meunier PJ, Roux C, Seeman E, Ortolani S, Badurski JE, Spector TD, Cannata J, Balogh A, Lemmel EM, Pors-Nielsen S, Rizzoli R, Genant HK and Reginster JY, The effects of strontium ranelate on the risk of vertebral fracture in women with postmenopausal osteoporosis, New Engl J Med, 350, 459-468, 2004.

Mohini G Jagan, Krishnamacharyulu N, Baskaran G Sahaya, Rao P Venkateswara and Veeraiah N, Studies on influence of aluminium ions on the bioactivity of B_2O_3–SiO_2–P_2O_5–Na_2O–CaO glass system by means of spectroscopic studies, Appl Surf Sci, 287, 46–53, 2013.

Ni GX, Lu WW and Chiu KY, Strontium-containing hydroxyapatite (Sr-HA) bioactive cement for primary hip replacement: an in vivo study, J Biomed Mater Res B Appl Biomater, 77, 409-415, 2006.

O'Donnell S, Cranney A, Wells GA, Adachi JD and Reginster JY, Strontium ranelate for preventing and treating postmenopausal osteoporosis, Cochrane Database of Systematic Reviews, (3), CD005326, DOI: 10.1002/ 14651858.CD005326.pub2, 2006.

O'Donnell MD, Fredholm Y, Rouffignac A de and Hill RG, Structural analysis of a series of strontium-substituted apatites, Acta Biomater, 4, 1455–1464, 2008.

O'Donnell MD and Hill RG, Influence of strontium and the importance of glass chemistry and structure when designing bioactive glasses for bone regeneration, Acta Biomater, 6, 2382–2385, 2010.

O'Donnell MD, Candarlioglu PL, Miller CA, Gentleman E and Stevens MM, Materials characterization and cytotoxic assessment of strontium-substituted bioactive glasses for bone regeneration, J Mater Chem, 20, 8934–8941, 2010.

Ohtsuki C, Kokubo T and Yamamuro T, Compositional dependence of bioactivity of glasses in the system $CaO–SiO_2–Al_2O_3$: its in vitro evaluation, Journal of Materials Science: Materials in Medicine, 3, 119–125, 1992.

Rajendran V, Nishara Begum A, Azooz MA and El Batal FH, Microstructural dependence on relevant physical-mechanical properties on SiO_2-Na_2O-CaO-P_2O_5 biological glasses, Biomaterials, 23, 4263–4275, 2002.

Reginster JY, Felsenberg D, Boonen S, Diez-Perez A, Rizzoli R, Brandi ML, Spector TD, Brixen K, Goemaere S, Cormier C, Balogh A, Delmas PD and Meunier PJ, Effects of long-term strontium ranelate treatment on the risk of nonvertebral and vertebral fractures in postmenopausal osteoporosis: Results of a five-year, randomized, placebo-controlled trial, Arthritis Rheum, 58, 1687-1695, 2008.

Romeis S, Hoppe A and Eisermann C, Enhancing *In Vitro* Bioactivity of Melt-Derived 45S5 Bioglass ® by Comminution in a Stirred Media Mill, J Am Ceram Soc, 97, 150–156, 2014.

Sampath Kumar Arepalli, Tripathi Himanshu, Vyas Vikash Kumar, Kumar S Shyam, Jain Shubham, Pyare Ram and Singh SP, Influence of barium substitution on bioactivity, thermal and physico-mechanical properties of bioactive glass, Material Science and Engineering C, 49, 549-559, 2015.

Silver IA, Deas J and Erecińska M, Interactions of bioactive glasses with osteoblasts in vitro: effects of 45S5 Bioglass®, and 58S and 77S bioactive glasses on metabolism, intracellular ion concentrations and cell viability, Biomaterials, 22, 175-185, 2001.

Sitarz M, Bulat K and Szumera M, Aluminium influence on the crystallization and bioactivity of silico-phosphate glasses from $NaCaPO_4$–SiO_2 system, Journal of Non-Crystalline Solids, 356, 224–231, 2010.

Tai BJ, Bian Z, Jiang H, Greenspan DC, Zhong J and Clark AE, Anti-gingivitis effect of a dentifrice containing bioactive glass (NovaMin (R)) particulate, J Clin Periodontol, 33, 86–91, 2006.

Towler MR, Crowley CM, Murphy D and O'Callaghan AMC, A preliminary study of an aluminium-free glass polyalkenoate cement, J Mater Sci Lett, 21, 1123–1126, 2002.

Vallet-Reg M, Romn J and Padilla S, Bioactivity and mechanical properties of SiO_2-CaO-P_2O_5 glass-ceramics, J Mater Chem, 15, 1353, 2005.

Verne E, Nunzio S Di, Bosetti M, Appendino P, Brovarone C Vitale, Maina G and Cannas M, Surface characterization of silver-doped bioactive glass, Biomaterials, 26, 5111–5119, 2005.

Wong CT, Lu WW and Chan WK, *In vivo* cancellous bone remodeling on a strontium containing hydroxyapatite (sr-HA) bioactive cement, J Biomed Mater Res A, 68, 513–521, 2004.

Wu C, Zhou Y and Lin C, Strontium-containing mesoporous bioactive glass scaffolds with improved osteogenic/cementogenic differentiation of periodontal ligament cells for periodontal tissue engineering, Acta Biomater, 8, 3805–3815, 2012.

Wu C and Chang J, Multifunctional mesoporous bioactive glasses for effective delivery of therapeutic ions and drug/growth factors, J Control Release, 193, 282–295, 2014.

Zhao Di, Huang Wenhai, Rahaman Mohamed N, Day Delbert E and Wang Deping, Mechanism for converting Al_2O_3-containing borate glass to hydroxy apatite in aqueous phosphate solution, Acta Biomater, 5, 1265–1273, 2009.